Pathogenesis of Pneumococcal Pneumonia in Cyclophosphamide-Induced Leukopenia in Mice

Erjian Wang, Marie Simard, Nathalie Ouellet, Yves Bergeron,
Denis Beauchamp, and Michel G. Bergeron*

Infectious Diseases Research Center, Laval University, Quebec City, Quebec, Canada G1V 4G2

Streptococcus pneumoniae pneumonia frequently occurs in leukopenic hosts, and most patients subsequently develop lung injury and septicemia. However, few correlations have been made so far between microbial growth, inflammation, and histopathology of pneumonia in specific leukopenic states. In the present study, the pathogenesis of pneumococcal pneumonia was investigated in mice rendered leukopenic by the immunosuppressor antineoplastic drug cyclophosphamide. Compared to the immunocompetent state, cyclophosphamide-induced leukopenia did not hamper interleukin-1 (IL-1), IL-6, macrophage inflammatory protein-1 (MIP-1), MIP-2, and monocyte chemotactic protein-1 secretion in infected lungs. Leukopenia did not facilitate bacterial dissemination into the bloodstream despite enhanced bacterial proliferation into lung tissues. Pulmonary capillary permeability and edema as well as lung injury were enhanced in leukopenic mice despite the absence of neutrophilic and monocytic infiltration into their lungs, suggesting an important role for bacterial virulence factors and making obvious the fact that neutrophils are ultimately not required for lung injury in this model. Scanning and transmission electron microscopy revealed extensive disruption of alveolar epithelium and a defect in surfactant production, which were associated with alveolar collapse, hemorrhage, and fibrin deposits in alveoli. These results contrast with those observed in immunocompetent animals and indicate that leukopenic hosts suffering from pneumococcal pneumonia are at a higher risk of developing diffuse alveolar damage.

Severe pulmonary infections and bacteremia frequently occur in leukopenic patients, since leukocytes are primary mediators of pulmonary host defense in response to invading pathogens (3, 18, 37). The high mortality rate in leukopenic patients occurs at an early stage of the infection and has been associated with signs and symptoms that resemble those in acute respiratory distress syndrome (ARDS) observed in immunocompetent persons (1, 31, 33, 34, 35, 43, 48). Leukopenia is also a common complication of modern aggressive anticancer chemotherapy, and *Streptococcus pneumoniae* is the causative agent of an increasing number of pulmonary infections in cancer patients (10). Nevertheless, the pathogenesis of pneumococcal pneumonia and lung injury in leukopenic hosts receiving cytotoxic chemotherapy remains poorly studied.

The goal of the present study was to characterize lung injury in relation to host response to pneumococcal pneumonia in immunocompetent versus cyclophosphamide-induced leukopenic mice. We hypothesized that differences in the kinetics of bacterial growth and of cytokine and chemokine expression as well as of neutrophil and monocyte/macrophage emigration into lung tissue of leukopenic versus immunocompetent mice would promote different histopathologic features of lung injury in severe *S. pneumoniae* pneumonia. A better understanding of the pathogenesis of pneumonia in leukopenic host is not only of theoretical interest but also of therapeutic significance.

MATERIALS AND METHODS

Pneumonia model. Infection was induced in lightly anesthetized (isoflurane) immunocompetent and immunosuppressed female CD1 Swiss mice (18 to 20 g) by intranasal instillation of 50 μl of a 10^7-CFU-containing suspension of a clinically isolated *S. pneumoniae* serotype 3 strain, as already described (7, 14, 15, 16, 40, 49, 50). Leukopenia was induced by intraperitoneal injections of cyclophosphamide (150 mg/kg of body weight; Charte-Horner Inc., Mississauga, Ontario, Canada) 3 successive days before and 1 day after bacterial challenge.

Experimental protocol. Twenty-four infected leukopenic or immunocompetent mice were used for daily recording of survival rates. Additional immunocompetent and leukopenic-rendered mice were also infected for pathogenesis studies. To this end, 14 animals per group per time were sacrificed by CO_2 inhalation either before infection or at 4, 24, 48, 72, or 96 h after infection. Blood, lungs, and bronchoalveolar lavage (BAL) fluids were obtained and processed as already described (7, 14, 15, 16, 40, 49, 50). End points included bacterial growth, release of cytokines and chemokines, leukocyte emigration into lung interstitium and alveolar spaces (five mice per group per time point), histology (two mice per group per time point for light and transmission electron microscopy and two mice per group per time point for scanning electron microscopy), as well as pulmonary vascular permeability and edema (5 mice per group per time point; those mice were not exsanguinated).

Bacterial growth. Serial 10-fold dilutions of lung homogenates and blood were plated on blood agar to determine bacterial growth and bacteremia. The limit of detection was 2 $\log_{10}$ CFU per ml of lung homogenate or blood.

Leukocyte recruitment. Leukocyte populations in blood were quantified using a Coulter counter. The infiltration of neutrophils into pulmonary interstitium was evaluated by the myeloperoxidase (MPO) (an intracellular enzyme specific for neutrophils) activity in lung homogenates after removal of residual blood from lungs (7). Leukocyte populations that emigrated into alveoli were distinguished and quantified in BAL fluid, as already described (7).

Inflammatory mediators. The cytokines evaluated, including tumor necrosis factor alpha, interleukin-1β (IL-1β), and IL-6, and the chemokines which are chemoattractant for neutrophils (macrophage inflammatory protein-2 [MIP-2]) or for monocytes/macrophages (MIP-1α and monocyte chemotactic protein-1 [MCP-1]) were all quantified by sandwich enzyme-linked immunosorbent assay in the supernatants of lung homogenates after addition of aprotinin and 3-[(3-cholamidopropyl)-dimethylammonio]-1-propanesulfonate (CHAPS), as already described (7, 16). The release of nitric oxide (NO) in BAL fluids was evaluated

* Corresponding author. Mailing address: Infectious Diseases Research Center, CHUQ, CHUL Building, 2705 Laurier Blvd, Sainte-Foy, Quebec, Canada G1V 4G2. Phone: (418) 654-2705. Fax: (418) 654-2715. E-mail: Michel.G.Bergeron@crchul.ulaval.ca.

by the colorimetric method of Griess after reduction of nitrate into nitrite metabolites (7).

Histopathology. Lungs were perfused with saline, and left lobes were fixed in buffered 10% formalin and then embedded in Paraplast. Five-micrometer-thick sections were stained with hematoxylin-eosin for light microscopy. Small parts of the upper right lobes were fixed in 2.5% glutaraldehyde in phosphate buffer and postfixed in 1% osmium tetroxide for electron microscopy. They were embedded in Epon and sectioned for transmission electron microscopy (JEOL 1010 microscope), or metalized with gold for scanning electron microscopy (JEOL JSM 35 CF microscope). At least four tissue sections representing various areas of the lobes of representative mice were examined for each infected and uninfected group at every time point. Control animals receiving placebo or cyclophosphamide were examined at the same time points. A scoring grid was established to approximate histopathology, it was based on semiquantitative analysis of microscopic alterations and lung injury. Criteria included leukocytes in lungs, vascular injury, surfactant in alveoli, necrosis near blood vessels, intra-alveolar fibrosis, and collapsed alveoli, which were graded from 0 (none) to 1 (scarce), 2 (mild), 3 (moderate), or 4 (severe) based on severity of signs of injuries or extent of modifications compared to uninfected controls.

Pulmonary vascular permeability and edema. Evans blue avidly binds to serum albumin and can be used as a tracer for transcapillary flux of macromolecules (26). Evans blue was injected through a vein of the tail 30 min before sacrifice. Lungs were homogenized in 2 ml of potassium phosphate buffer. Evans blue was extracted by incubating samples in 4 ml of formamide at 60°C for 24 h. After centrifugation at $5,000 \times g$ for 30 min, Evans blue was quantified in supernatants by absorption at 620 and 740 nm. Correction for contaminating heme pigments was calculated as follows: E_{620} (corrected) = $E_{620} - (1.426 \times E_{740} + 0.030)$. Edema was observed through weight changes and final wet/dry ratio after desiccation of unperfused lungs at 60°C for 24 h.

Statistical analyses. Data are shown as means ± standard deviations (SD) for five mice per group per time point in all assays. A Student t test was used to compare immunocompetent and immunosuppressed mice at specific time points. Two mice per infected and uninfected immunocompetent and immunosuppressed groups were used for light and transmission electron microscopy at each time point, and two additional mice per group per time point were used for scanning electron microscopy. At least four tissue sections representing various areas of the lobes were examined for each individual mouse.

RESULTS

Survival rates. Infected immunocompetent and leukopenic animals exhibited similar signs of sickness: lethargy and then ruffled fur, by 4 h and 1 day postinfection, respectively. By day 2, all leukopenic mice developed progressive respiratory distress (laborious breathing and cyanosis) by contrast to immunocompetent animals. Fifty percent and 100% of leukopenic mice were dead by the end of days 2 (60 h) and 3 (84 h) postinfection, respectively, while 50 and 100% of immunocompetent mice were dead by the end of days 3 (84 h) and 4 (108 h).

Bacterial growth in lungs and blood. Bacterial counts in lung homogenates and blood are presented in Fig. 1. Although similar counts were observed in lungs of both immunocompetent and leukopenic mice 4 h after infection, bacterial growth occurred more rapidly and to a greater extent thereafter in leukopenic mice (Fig. 1A). In fact, significantly higher counts were noted in leukopenic mice from 24 to 72 h (P, <0.05, <0.001, and <0.01 at 24, 48, and 72 h, respectively), while a gradual increase was observed in lungs of immunocompetent mice from 24 to 96 h postinfection. However, leukocyte depletion did not facilitate bacterial dissemination and proliferation into the bloodstream. No bacteria were detected in blood of either group at 4 h postinfection. Septicemia developed in 42% (three of seven) and 100% (seven of seven) of animals from both infected groups on days 1 and 2 postinfection, respectively. As for the log_{10} CFU in positive blood cultures (Fig.
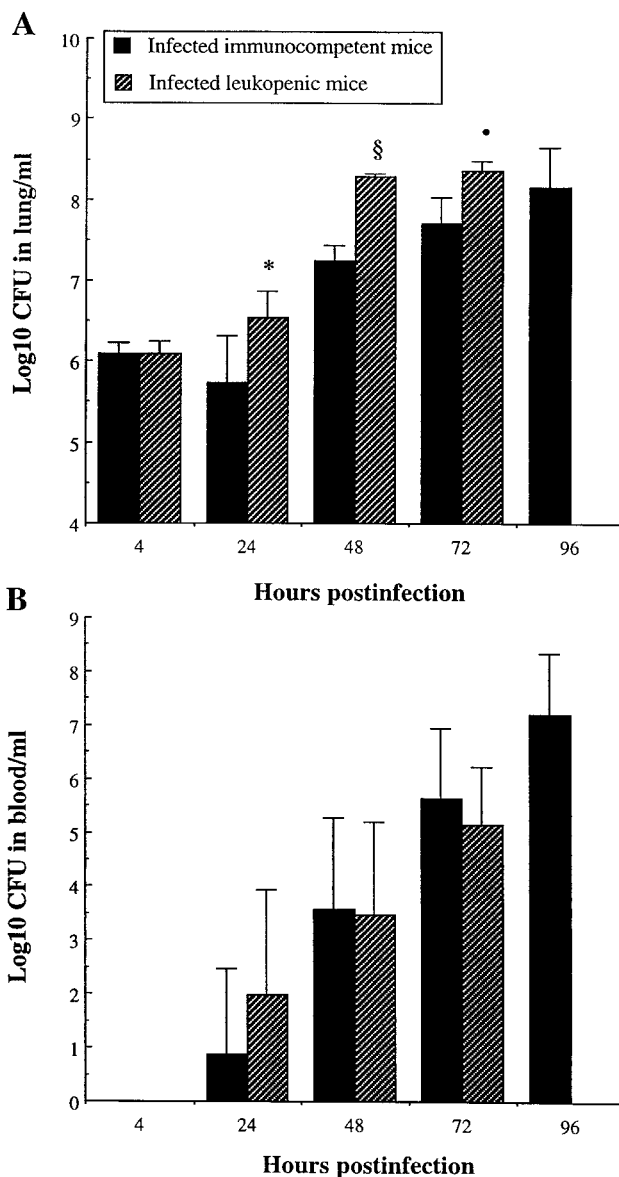

FIG. 1. Bacterial counts in lungs (A) and bloodstream (B) of immunocompetent and leukopenic mice infected with *S. pneumoniae* (means + SD [error bars] for five mice). Values that were significantly greater than those observed for infected immunocompetent mice are indicated by symbols as follows: $*$, $P < 0.05$; $\bullet$, $P < 0.01$; §, $P < 0.001$.

1B), it increased gradually from 24 h until death of the animals without any significant difference between the two groups ($P > 0.05$).

Leukocyte recruitment. Cyclophosphamide injections depleted blood leukocytes of uninfected mice from 7.2×10^9 to 1.0×10^9 cells/liter throughout the experiment. Infection with *S. pneumoniae* resulted in early but transient cell influx in the bloodstream of immunocompetent mice (peak of 13×10^9 cells/liter at 4 h) (Fig. 2). The level of white blood cells (WBCs) in infected leukopenic animals was below 2×10^9 cells/liter at 4 h postinfection and remained lower than 1×10^9 cells/liter throughout the rest of the experiment. Significant differ-
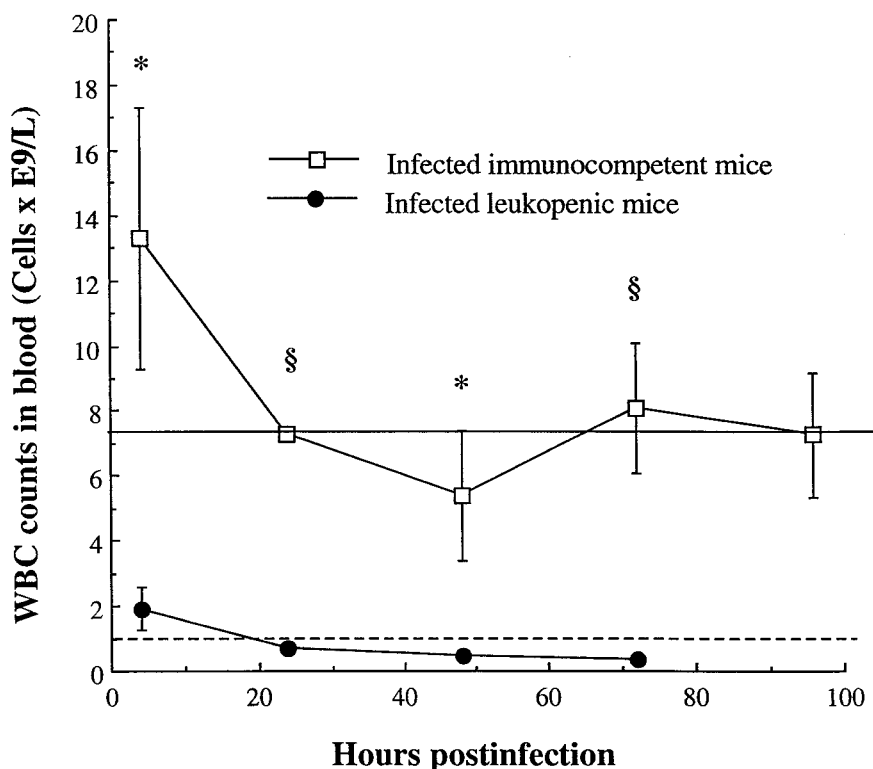
FIG. 2. WBCs in peripheral bloodstream of immunocompetent and leukopenic mice infected with *S. pneumoniae* (means ± SD [error bars] for five mice). Values that were significantly greater than those observed for infected leukopenic mice are indicated by symbols as follows: *, $P < 0.05$; §, $P < 0.01$. Cyclophosphamide injections resulted in blood leukocyte depletion from 7.2×10^9 cells/liter (pretreatment, straight line) to 1.0×10^9 cells/liter (throughout the experiment, dotted line) in uninfected control mice.

ences in WBC counts were observed between the two infected groups at each time point throughout the experiment (from $P < 0.05$ to $P < 0.001$).

Polymorphonuclear leukocyte (PMN) recruitment into lung tissues was quantified by the MPO activity in lung homogenates (Fig. 3). MPO activity in uninfected immunocompetent and leukopenic mice was close to zero, suggesting that neutrophils were merely absent from lung interstitium. Infection of immunocompetent mice rapidly ($P < 0.001$ at 4 h) and significantly enhanced MPO throughout the experiment, indicating strong PMN emigration into tissues. No such increase was observed in leukopenic mice, with MPO levels remaining at basic values similar to those observed in uninfected animals.

Alveolar macrophages were the predominant resident leukocytes in alveolar spaces (BAL fluids) of noninfected animals, and only scarce neutrophils could be recovered from that site. Infection rapidly triggered neutrophil recruitment (Fig. 4C) and then monocyte/macrophage emigration (Fig. 4B) into alveoli of immunocompetent mice, resulting in high leukocyte counts in BAL fluid throughout the evolution of pneumonia (Fig. 4A). Cyclophosphamide effectively prevented both PMN and monocyte/macrophage recruitment. The kinetics of PMNs in BAL fluid nearly paralleled that of MPO in lungs, which was further confirmed by light and electron microscopy observations.

Inflammatory mediators. High secretion of IL-1β, IL-6, MIP-2, MIP-1α, and MCP-1 was noted in lung homogenates of

both immunocompetent and leukopenic mice after infection with *S. pneumoniae* (Fig. 5). Comparative analysis showed no significant difference in any cytokine or chemokine levels between immunocompetent and leukopenic mice at any time point. Hence, leukocyte depletion by cyclophosphamide had no effect on pulmonary levels of the studied proinflammatory cytokines and chemokines despite large differences in the kinetics of neutrophils and monocytes/macrophages. By contrast, Fig. 6 shows that NO production was significantly reduced in lungs of leukopenic infected mice compared to that in immunocompetent infected animals from 24 to 72 h postinfection ($P < 0.05$).

Pulmonary vascular permeability. We evaluated the vascular endothelium integrity by the Evans blue permeability assay. A higher ($P < 0.05$) pulmonary vascular permeability index was observed in infected immunocompetent mice than that in leukopenic mice as early as 4 h postinfection (Fig. 7). By contrast, higher vascular permeability was observed in lungs of infected leukopenic mice later on, reaching greater values than those in immunocompetent animals by 48 h postinfection ($P < 0.05$). Optical density values for uninfected immunocompetent versus leukopenic mice were, respectively, 1.64 ± 0.10 versus 1.60 ± 0.14, suggesting that cyclophosphamide itself had no direct effect on epithelial and endothelial integrity and in the setting of an inflammatory stimulus.

Lung edema. A higher and gradually increasing wet/dry lung weight ratio was observed from day 1 to 3 in infected leuko-
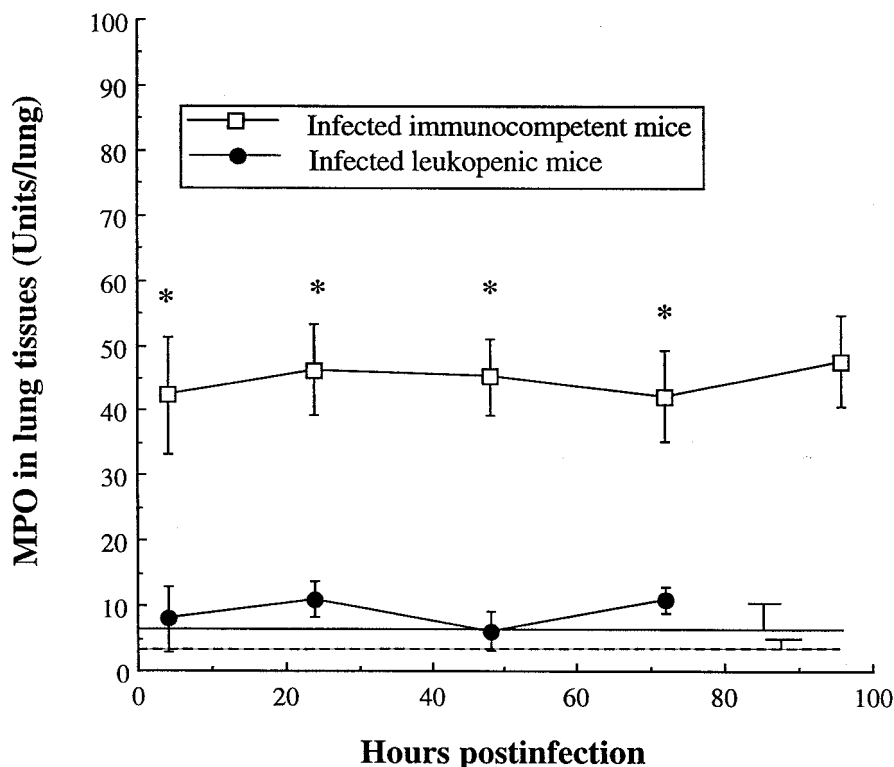
FIG. 3. MPO in lungs of immunocompetent and leukopenic mice infected with *S. pneumoniae* (means ± SD [error bars] for 5 mice). Levels in uninfected immunocompetent and leukopenic mice were, respectively, 6 ± 4 (straight line) and 4 ± 1 U/lung (dotted line). *, $P < 0.001$ (value was significantly greater than that observed for infected leukopenic mice).

penic mice compared to that in infected immunocompetent animals ($P < 0.01$, $P < 0.001$, and $P < 0.001$ from 24 to 48 to 72 h, respectively (Fig. 8).

Histopathology. Structural and ultrastructural examination of lungs was made by light microscopy (Fig. 9), as well as by scanning (Fig. 10) and transmission electron microscopy (Fig. 11). The main pneumonia feature noted in immunocompetent mice was a progressive infiltration of leukocytes in interstitial and alveolar spaces (Fig. 9A). Extensive peribronchial inflammatory exudation also expanded through adjacent alveoli (Fig. 9A). Scanning electron microscopy showed intensive extravasation of polymorphonuclear cells (Fig. 10B), macrophages (Fig. 10C), and red blood cells (Fig. 10B and C) in alveoli. Furthermore, collapsed alveoli were observed in these mice (Fig. 10B and C) compared to the noninfected immunocompetent mice (Fig. 10A). Transmission electron microscopy revealed alveoli filled with edema, red blood cells, and surfactant (Fig. 11A and B). Endothelial lining of capillaries and epithelial basement membrane became dilated, vacuolated, and discontinued, as seen by high magnification (Fig. 11B).

The typical pathological feature of pneumonia that occurred in leukopenic mice was not similar to that seen in immunocompetent mice. There was no leukocyte infiltration either in the interstitium or alveolar spaces (Fig. 9C). Yet, intensive damage to elastic tissues resulted in coarse and dense masses that were formed in alveolar spaces and walls (Fig. 9C). Scanning electron microscopy revealed numerous bacteria (Fig. 10, left part of E) and extravasation of red blood cells (Fig. 10, right part of E) in alveoli. Transmission electron microscopy showed dilated, vacuolated, and discontinued endothelial lining of alveolar capillaries (Fig. 11, the right part of E) as well as denudation, disruption, and complete destruction of endothelial cells (Fig. 11, the left part of E). Wide sections of disrupted epithelial cells and complete loss of epithelial cells were more apparent in leukopenic (Fig. 11D) than in immunocompetent animals. Alveolar edema (constituted of fluid and debris) was more severe in leukopenic than in immunocompetent animals, but surfactant was scarcely observed in alveoli of leukopenic animals. The most-striking structural change in leukopenic animals was extensive fibrosis in alveoli (Fig. 9C, 10F, and 11 the right part of E). Also, alveolar spaces were partially or completely obliterated, and collapsed alveolar spaces underwent fusion or coalescence.

Global morphological analysis of lung injury induced by pneumococcal pneumonia in leukopenic and immunocompetent states is summarized in Table 1. It was clear that leukocytes in lungs, tissue injury, and overproduction of surfactant characterized the pathogenesis of pneumonia in immunocompetent mice. By contrast, an absence of leukocytes in leukopenic mice was associated with more-severe alveolar epithelial cell injury and fibrotic deposits as well as numerous collapsed alveoli but was associated with a striking absence of surfactant secretion compared to immunocompetent infected mice.
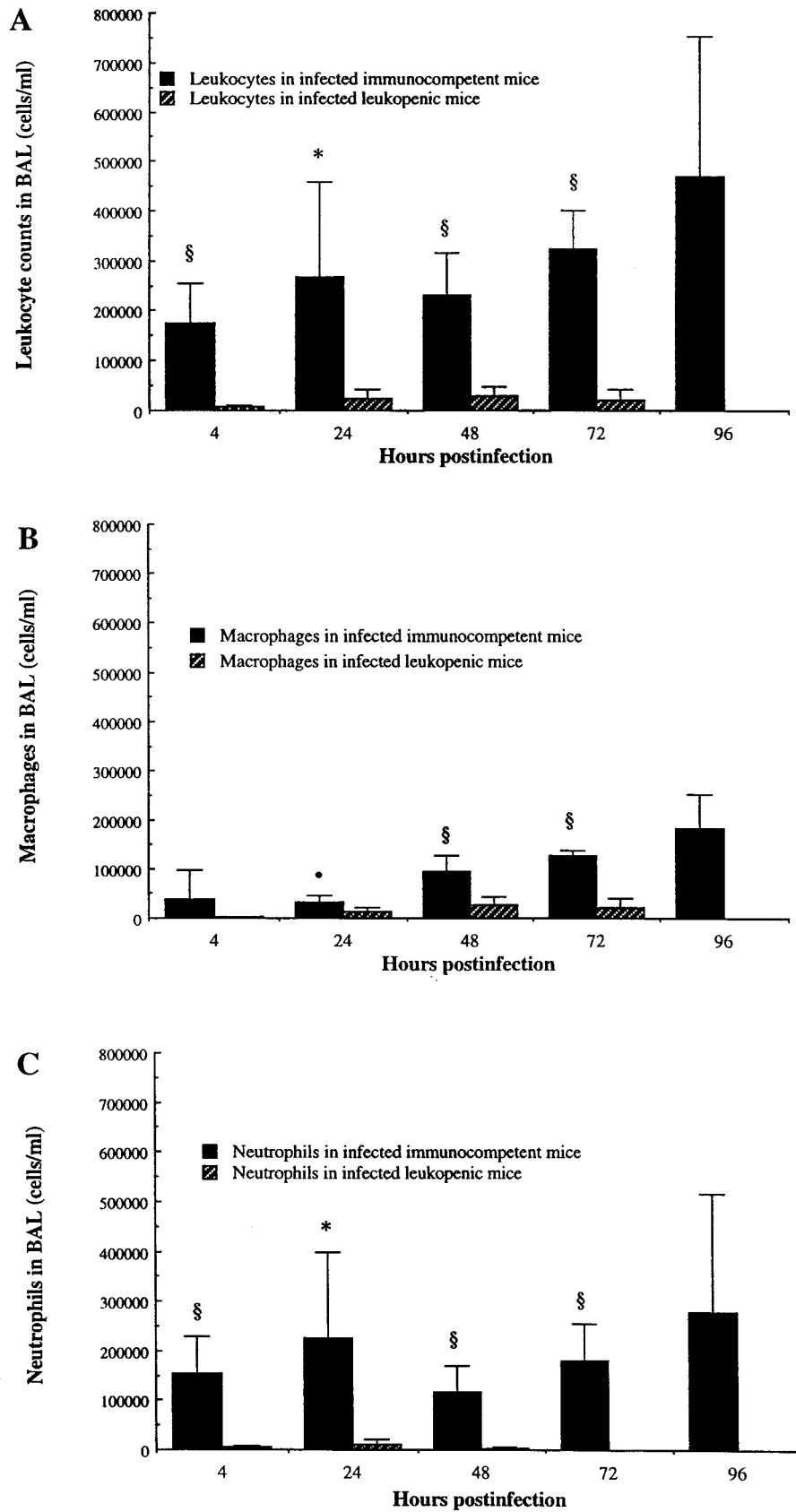
FIG. 4. Leukocyte counts in BAL fluids of immunocompetent and leukopenic mice infected with *S. pneumoniae* (means + SD [error bars] for five mice). Values that were significantly greater than those observed for infected leukopenic mice are indicated by symbols as follows: ∗, $P < 0.01$; ●, $P < 0.05$; §, $P < 0.001$. Values of total leukocytes, macrophages, and neutrophils in BAL fluids of uninfected mice were, respectively, $1.3 \times 10^4 \pm 0.71 \times 10^4$, $1.3 \times 10^4 \pm 0.71 \times 10^4$, and 0 cells/ml for both immunocompetent and leukopenic mice.
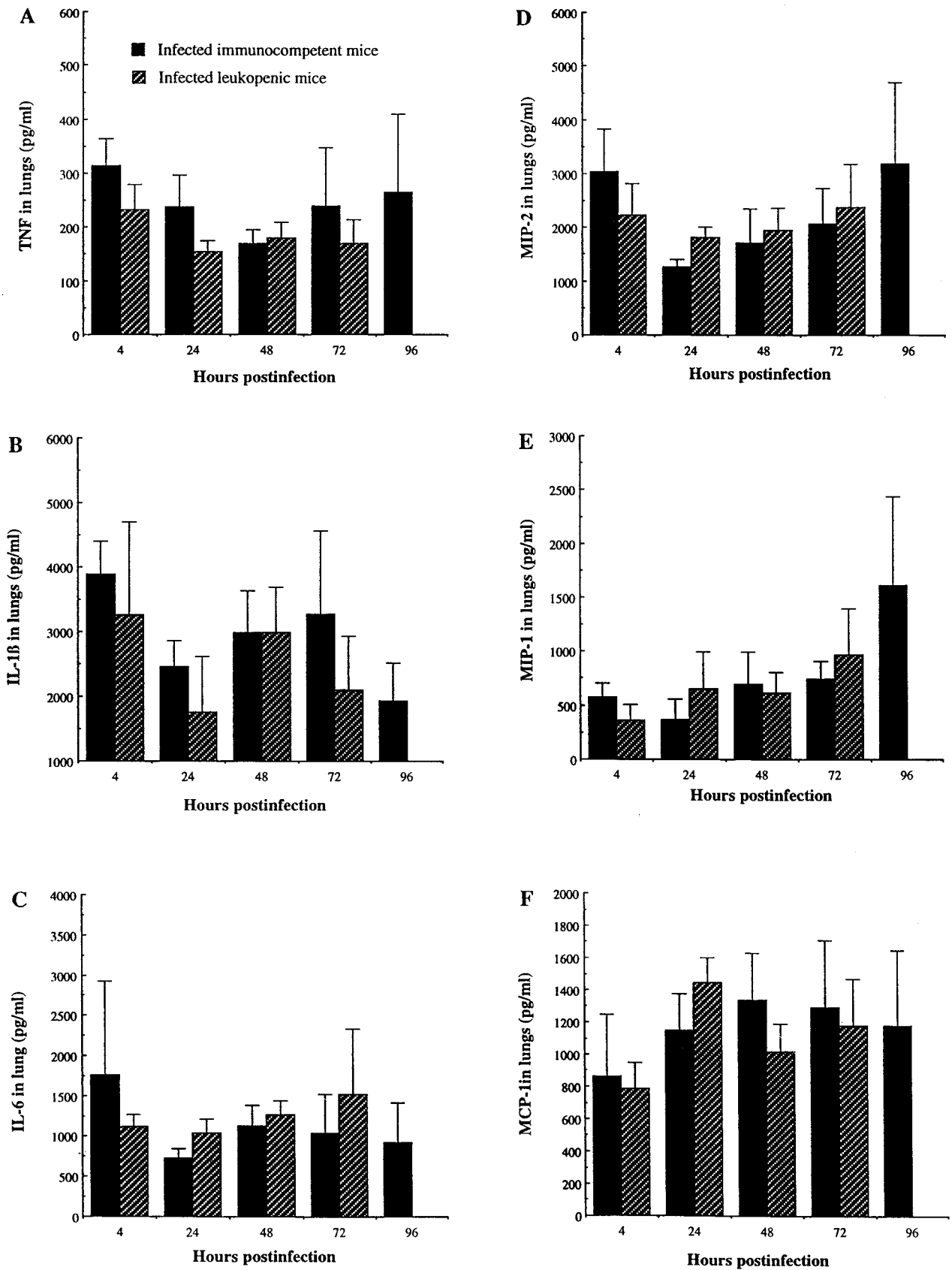
FIG. 5. Levels of proinflammatory cytokines and chemokines in lungs of immunocompetent and leukopenic mice infected with *S. pneumoniae* (means + SD [error bars] for five mice). Values of tumor necrosis factor (TNF), IL-1, IL-6, MIP-2, and MIP-1 for uninfected immunocompetent versus leukopenic mice were, respectively, 200 ± 10 and 160 ± 15, $1,600 \pm 100$ and $1,500 \pm 200$, 700 ± 50 and 450 ± 250, 700 ± 200 and 450 ± 400, and 100 ± 100 and 100 ± 100. MCP-1 values for both uninfected groups were below the limit of detection of the assay, which was between 20 and 500 pg/ml.
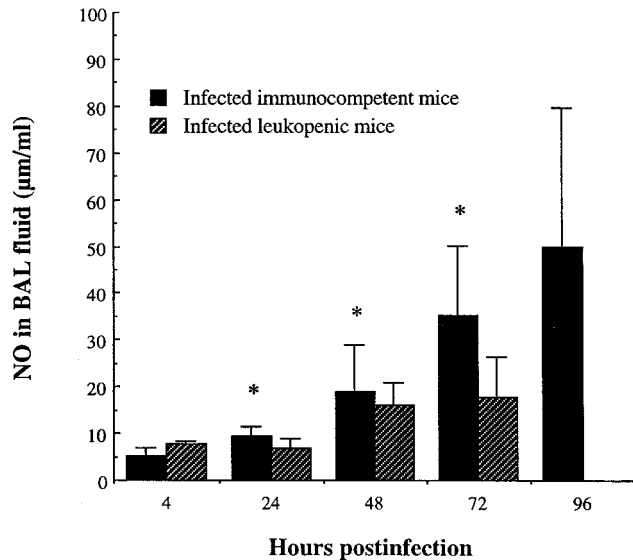
FIG. 6. Levels of nitric oxide (NO) in BAL fluids of immunocompetent and leukopenic mice infected with *S. pneumoniae* (means + SD [error bars] for five mice). Values for uninfected immunocompetent versus leukopenic animals were, respectively, 10 ± 2 and 9 ± 2 μm/ml. *, value was significantly greater than that for infected leukopenic mice ($P < 0.05$).
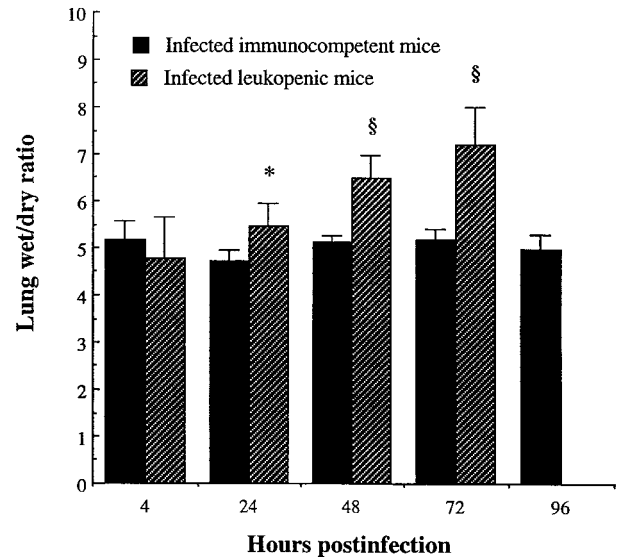

FIG. 8. Wet/dry lung weight ratio for immunocompetent and leukopenic mice infected with *S. pneumoniae* (means + SD [error bars] for five mice). Values that were significantly greater than those observed for infected immunocompetent mice are indicated by symbols as follows: *, $P < 0.01$; §, $P < 0.001$. Values for uninfected immunocompetent versus leukopenic mice were, respectively, 4.4 ± 0.2 and 4.2 ± 0.2.

DISCUSSION

The goal of the present study was to investigate simultaneously host defense mechanisms and pulmonary injuries that together characterize pneumococcal pneumonia in leukopenic
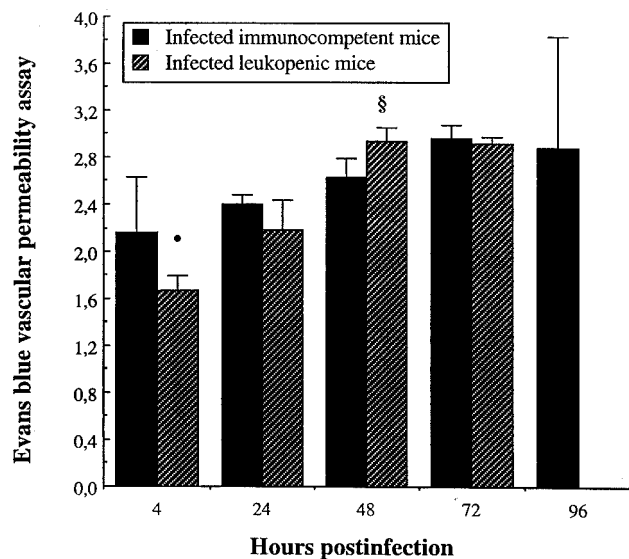

FIG. 7. Pulmonary vascular permeability of immunocompetent and leukopenic mice infected with *S. pneumoniae* (means + SD [error bars] for five mice). Values for uninfected immunocompetent versus leukopenic mice were, respectively, of 1.64 ± 0.10 versus 1.60 ± 0.14. Symbols: ●, $P < 0.05$ (value was significantly lower than that for infected immunocompetent mice); §, $P < 0.05$ (value was significantly greater than that for infected immunocompetent mice).

states, by comparison to those that prevail in immunocompetent hosts.

Although our results suggest a critical role for neutrophils and monocytes on pneumococcal clearance from the lungs (since bacterial growth in lungs was enhanced in leukopenic mice), leukocyte depletion by cyclophosphamide did not facilitate dissemination of pneumococci from lungs into bloodstream, as shown by hemocultures. Therefore, lungs could be a more susceptible target than blood for pneumococci in cyclophosphamide-treated patients. In our recent study on sepsis (51), leukocyte depletion by cyclophosphamide did not impair the early clearance of pneumococci from blood but facilitated growth in lungs. Actually, most neutropenic cancer patients with pneumococcal bacteremia suffer from pneumonia (8, 9, 11).

The magnitude and duration of the inflammatory process in lungs are considered to be important determinants of bacterial clearance but also of the severity of, and mortality from, pneumonia. Although a vigorous response by phagocytic cells at the early stage of infection is assumed to protect host from bacterial invasion, increasing evidence also suggests that persistent high levels of proinflammatory cytokines, chemokines, and nitric oxide play a prominent role in acute lung injury and ARDS (6). However, little is known on the production and role (either beneficial or detrimental) of proinflammatory cytokines, chemokines, and nitric oxide in infected lungs during leukopenia. Our results demonstrate that proinflammatory cytokine and chemokine levels in severely leukocyte-deprived lungs were consistently equivalent to those in lungs filled with leukocytes. It is likely that the production of such proinflammatory cytokines and chemokines in infected lungs was not dependent on the number of leukocytes in infected mice administered cyclo-
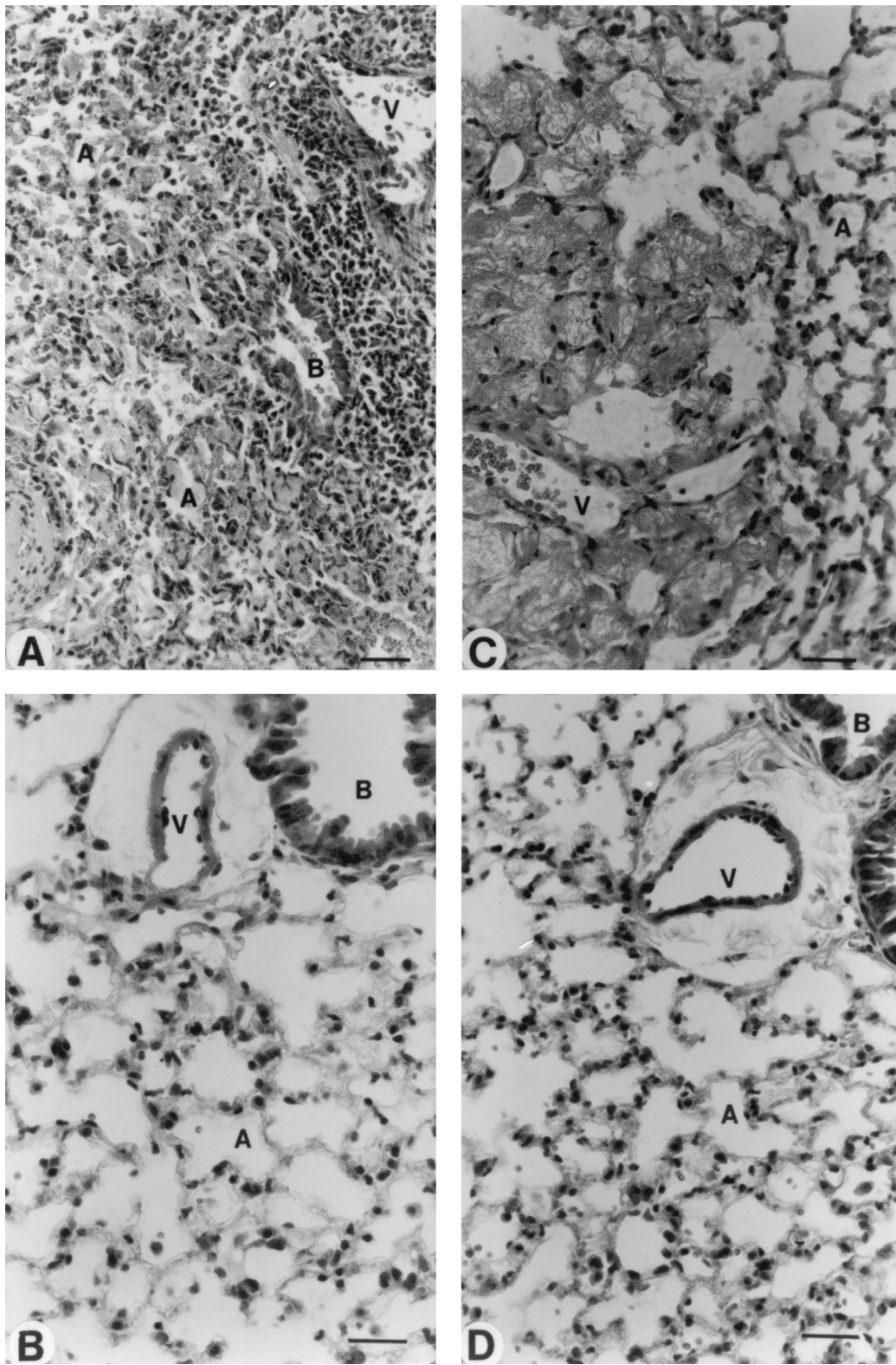
FIG. 9. Morphological analysis of lung tissues by light microscopy. Studies of infected immunocompetent (A) and leukopenic (C) mice were conducted on day 2 postinfection. Healthy lungs were observed in noninfected immunocompetent (B) and leukopenic (D) mice. Abbreviations: A, alveolar space; B, bronchiolus; V, blood vessel. Scale bar = 20 μm.
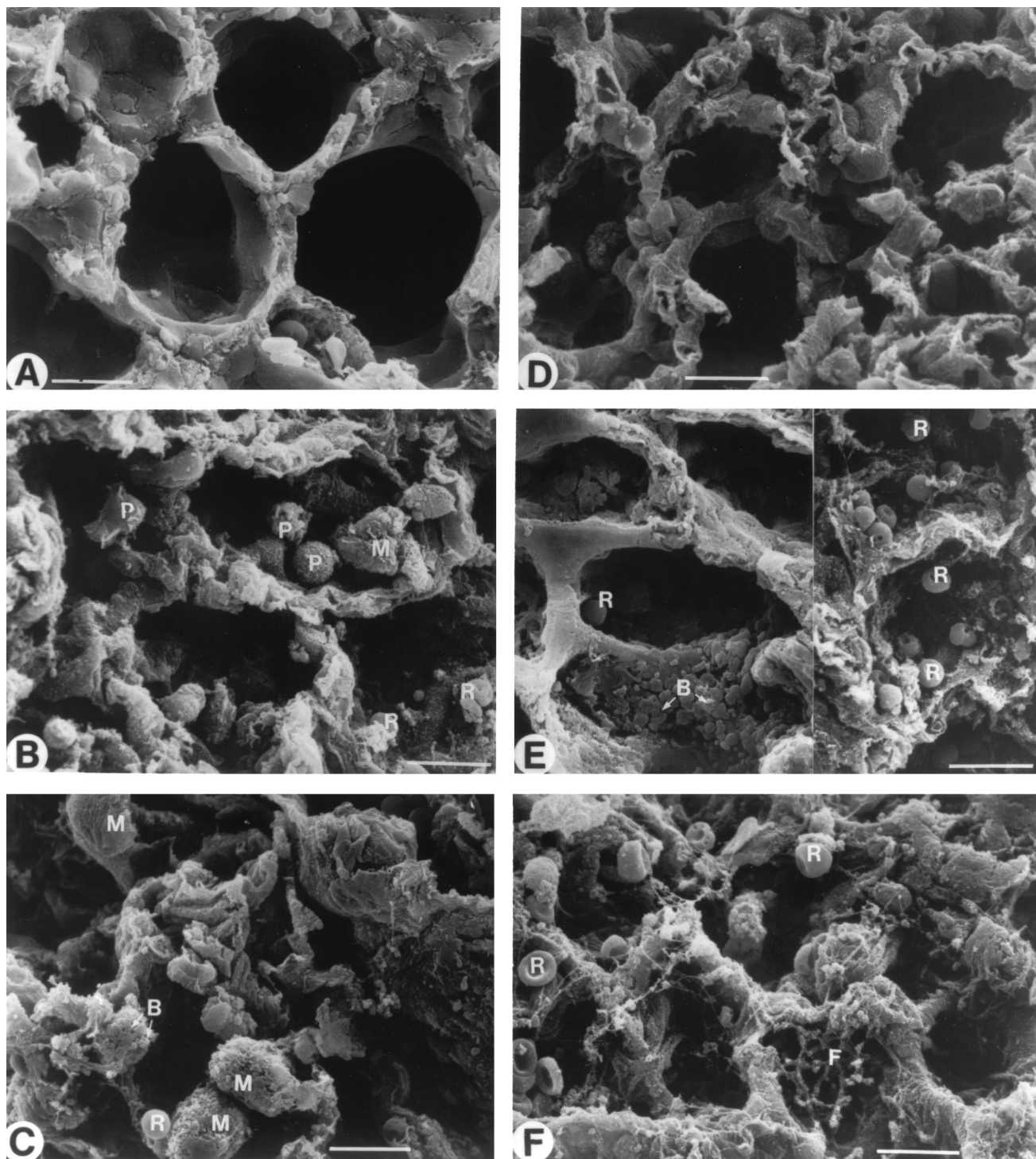
FIG. 10. Morphological analysis of lung tissues by scanning electron microscopy. Healthy lungs were observed in noninfected immunocompetent (A) and leukopenic (D) mice. Micrographs were taken of lungs from infected immunocompetent mice on days 2 (B) and 3 (C) postinfection and of lungs from infected leukopenic mice on days 2 (E) and 3 (F) postinfection. Abbreviations: B, bacteria; F, fibrosis; M, macrophage; P, polymorphonuclear cell; R, red blood cell. Scale bar = 10 μm.

phosphamide. In vitro studies indicate that alveolar epithelium and endothelium as well as pulmonary interstitial cells such as fibroblasts are capable of producing appreciable amounts of proinflammatory cytokines and chemokines upon stimulation with various agents (36, 42, 44, 45). Our in vivo study suggests that pulmonary parenchymal cells could be a rich source for inflammatory mediator release in leukopenic states, although we do not exclude that some undepleted resident alveolar
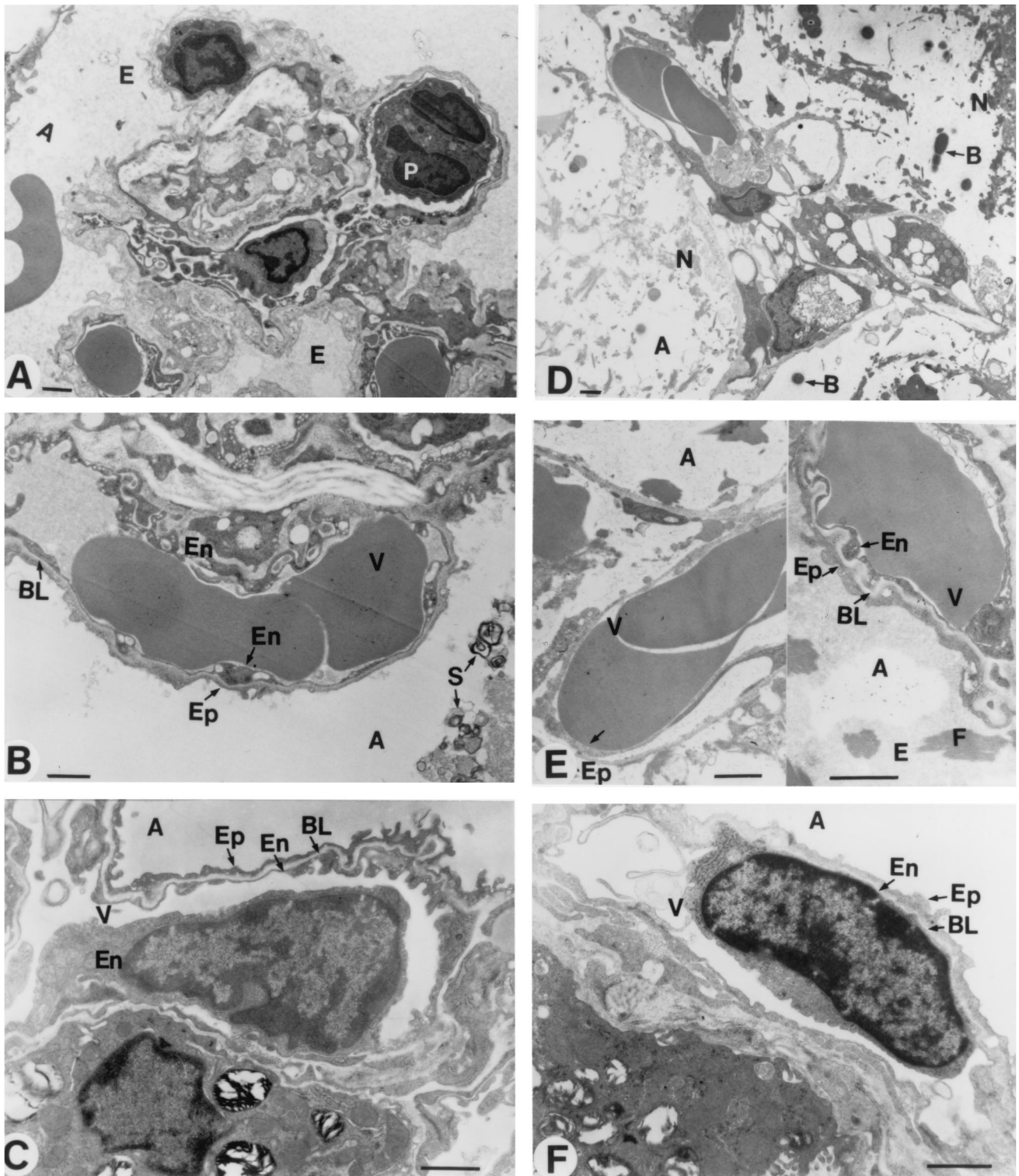
FIG. 11. Morphological analysis of lung tissues by transmission electron microscopy. Studies were conducted in infected immunocompetent (A and B) and leukopenic (D and E) mice on day 3 postinfection. Normal ultrastructure of endothelia and epithelia was observed in noninfected immunocompetent (C) and leukopenic (F) mice. Abbreviations: A, alveolar space; B, bacteria; BL, basal lamina; E, edema; En, endothelia; Ep, epithelia; F, fibrosis; N, necrotized tissue; P, polymorphonuclear cell; S, surfactant; V, blood vessel. Scale bar = 1 μm.

TABLE 1. Histopathology of lung injury in pneumococcal pneumonia in leukopenic and immunocompetent mice

Condition	Histopathological score[a] in mouse group at time (h)								
	Leukopenic				Immunocompetent				
	4	24	48	72	4	24	48	72	96
Leukocytes in lungs	0	0	0	0	1	2	3	4	4
Vascular injury	0	0	1	3	0	0	0	1	2
Surfactant in alveoli	0	0	1	0	0	1	2	3	4
Necrosis near the vessels	0	0	1	3	0	0	0	1	2
Intra-alveolar fibrosis	0	1	2	3	0	0	0	1	1
Collapsed alveoli	0	0	2	3	0	0	1	1	2

[a] Histopathological score (rates signs of injuries or extent of modifications compared to uninfected controls): 0, none; 1, scarce; 2, mild; 3, moderate; 4, severe.

macrophages may have accounted for cytokine production in both groups of animals. Lymphocytes are scarcely seen in lungs of mice over the first 3 days of infection in this model (7) and most likely did not generate the observed amounts of the studied cytokines and chemokines.

By contrast, leukocyte depletion significantly reduced nitric oxide release in BAL fluid during the late stage of pneumonia, suggesting that monocytes/macrophages recruited into the lungs could be a major source for NO production in pneumonia and that NO most likely participates in the killing of pneumococci.

At the early stage of pneumonia (4 h postinfection), the vascular permeability observed in the lungs of immunocompetent mice was higher than that observed in leukopenic animals. This result suggests that pulmonary vascular permeability was related to neutrophil activity (which differed greatly between immunocompetent and leukopenic mice) rather than to bacterial virulence factors at that time when bacterial counts did not differ between groups. This observation corroborates the limited pulmonary PMN infiltration and edema observed on radiographs of leukopenic patients at early stage of pneumonia (29). Animal models of endotoxemia suggest that PMNs are required for the development of vascular alterations (5, 17, 46), and it is generally believed that PMN adherence to pulmonary endothelium, with subsequent release of proteases, participate in pathological pulmonary microvascular permeability (2, 19, 20, 27, 41, 52, 53, 55).

By contrast, high vascular permeability and edema were observed at later stages of pneumonia in our model of leukopenic mice, at times when PMN counts were very low in lungs, suggesting that neutrophils are ultimately not required for lung injury in this model. These physiological data coincided with structural damage to pulmonary vascular endothelium, as noted by electron microscopy. We know from in vitro studies that pneumococcal cell wall may induce the separation of contiguous endothelial cells, which results in loss of the endothelial barrier function (22). Teichoic acid is known as an edema-inducing agent (13), and leakage of erythrocytes into alveoli has been reported in leukopenic states (38). In our experiment, bacterial toxins most likely contributed to endothelial cell injury and capillary leakage in leukopenic mice who experienced uncontrolled bacterial growth in lungs from 24 h to 72 h postinfection. The observed exudation of plasma and red blood cells into alveolar spaces of these mice and the high wet/dry lung weight ratio most likely reflected not only an increase in vascular permeability but also a greater alteration of alveolar

epithelium, as confirmed both by scanning and transmission electron microscopy. In fact, the alveolar epithelium is much less permeable to macromolecules than the endothelium (25). Epithelial cells have active transport mechanisms for the transfer of salt and water from the apical (airspace) to the basolateral (interstitial) compartment (12, 23, 24, 39). The integrity of these transport processes is critical for clearing fluids from the alveolar spaces. Injury and dysfunction to epithelial cells in leukopenic mice, along with compromised air-lung interface, may thus have exacerbated plasma leakage and/or alveolar hemorrhage in these animals.

Another feature of lung injury in our leukopenic pneumonia model was the presence of fibrin into the alveoli. It is clear that pneumococcal cell wall activates procoagulant activity at the surface of endothelial cells that is compatible with fibrin deposition seen during the "red hepatization" phase of pulmonary inflammation in human pneumonia (21). Our results corroborate other clinical and experimental observations that showed edema and fibrin deposition in lungs when bacterial multiplication was unchecked (54). Additional studies also reported significant intra-alveolar fibrosis following severe lung injury (4, 28, 30). The fibrotic deposits in alveoli of infected leukopenic animals in our experiment could result from the following mechanisms: First, they may result from the disruption of alveolar epithelial and endothelial membranes, with subsequent deposition of plasma proteins in alveolar spaces and finally the formation of fibrin and mesenchymal cell deposits. Therefore, fibronectin deposition in alveolar spaces would be a manifestation of plasma exudation and edema. Second, alveolar macrophages were observed engulfing and degrading extracellular material. Since alveolar macrophages are known to facilitate fibrosis dissolution (28), inhibition of macrophage recruitment in our experiment may at least in part have promoted accumulation of fibrotic material. Third, collagenase, an enzyme released by neutrophils, can extensively degrade the extracellular matrix. The absence of neutrophil recruitment and collagenase activity may have impaired digestion of fibrotic elements. The inability of leukopenic hosts to absorb fibrin may thus greatly contribute to increase intra-alveolar fibrosis.

It has been reported that edema and fibronectin deposits can induce death of experimental animals (54). Moreover, most patients who die from ARDS have morphological evidence of pulmonary fibrosis (4, 28, 30, 32, 47). Destruction of alveolar epithelial cell barriers and release of surfactant in alveolar spaces may thus have stimulated alveolar collapse, edema,

clotting and scarring processes, respiratory distress, and death, suggesting a predisposition of leukopenic hosts to undergo diffuse alveolar damage, in comparison to the pneumonia that develops in immunocompetent hosts.

Appropriate therapy of pneumonia in leukopenic hosts would theoretically benefit from the addition of an antitoxin drug that would control pulmonary injuries induced by bacterial components.

REFERENCES

1. **Anonymous.** 1987. Adult respiratory distress syndrome and neutropenia. N. Engl. J. Med. **316:**413–414.
2. **Arfors, K. E., C. Lundberg, L. Lindbom, K. Lundberg, P. G. Beatty, and J. M. Harlan.** 1987. A monoclonal antibody to the membrane glycoprotein complex CD18 inhibits polymorphonuclear leukocyte accumulation and plasma leakage in vivo. Blood **69:**338–340.
3. **Austrian, R., and J. Gold.** 1964. Pneumococcal bacteremia with especial reference to bacteremic pneumococcal pneumonia. Ann. Intern. Med. **60:**759–776.
4. **Bachofen, A., and E. R. Weibel.** 1977. Alterations of the gas exchange apparatus in adult respiratory insufficiency associated with septicemia. Am. Rev. Respir. Dis. **116:**589–615.
5. **Baird, B. R., J. C. Cheronis, R. A. Sandhaus, E. M. Berger, C. W. White, and J. E. Repine.** 1986. O2 metabolites and neutrophil elastase synergistically cause edematous injury in isolated rat lungs. J. Appl. Physiol **61:**2224–2229.
6. **Bergeron, Y., and M. G. Bergeron.** 1999. Why does pneumococcus kill? Can. J. Infect. Dis. **10**(Suppl. C)**:**49C-60C.
7. **Bergeron, Y., N. Ouellet, A. M. Deslauriers, M. Simard, M. Olivier, and M. G. Bergeron.** 1998. Cytokine kinetics and other host factors in response to pneumococcal pulmonary infection in mice. Infect. Immun. **66:**912–922.
8. **Bernard, C., G. Mombelli, and J. Klastersky.** 1981. Pneumococcal bacteremia in patients with neoplastic diseases. Eur. J. Cancer Clin. Oncol. **17:**1041–1046.
9. **Carratala, J., A. Marron, A. Fernandez-Sevilla, J. Linares, and F. Gudiol.** 1997. Treatment of penicillin-resistant pneumococcal bacteremia in neutropenic patients with cancer. Clin. Infect. Dis. **24:**148–152.
10. **Carratala, J., B. Roson, A. Fernandez-Sevilla, F. Alcaide, and F. Gudiol.** 1998. Bacteremic pneumonia in neutropenic patients with cancer: causes, empirical antibiotic therapy, and outcome. Arch. Intern. Med. **158:**868–872.
11. **Chou, M. Y., A. E. Brown, A. Blevins, and D. Armstrong.** 1983. Severe pneumococcal infection in patients with neoplastic disease. Cancer **51:**1546–1550.
12. **Cott, G. R., K. Sugahara, and R. J.** 1986. Mason. Stimulation of net active ion transport across alveolar type II cell monolayers. Am. J. Physiol. **250:**C222–C227.
13. **Cundell, D., H. R. Masure, and E. I. Tuomanen.** 1995. The molecular basis of pneumococcal infection: a hypothesis. Clin. Infect. Dis. **21**(Suppl. 3)**:**S204–S212.
14. **Dallaire, F., N. Ouellet, M. Simard, Y. Bergeron, and M. G. Bergeron.** 2001. Efficacy of recombinant human granulocyte colony-stimulating factor in a murine model of pneumococcal pneumonia: effects of lung inflammation and timing of treatment. J. Infect. Dis. **183:**70–77.
15. **Dallaire, F., Y. Bergeron, N. Ouellet, Y. Turmel, M. C. Gauthier, M. Simard, and M. G. Bergeron.** 2001. Microbiological and inflammatory factors associated with the development of pneumococcal pneumonia. J. Infect. Dis. **184:**292–300.
16. **Fillion, I., N. Ouellet, M. Simard, Y. Bergeron, S. Sato, and M. G. Bergeron.** 2001. Role of chemokines and formyl peptides in pneumococcal pneumonia-induced monocyte/macrophage recruitment. J. Immunol **166:**7353–7361.
17. **Flick, M. R., A. Perel, and N. C. Staub.** 1981. Leukocytes are required for increased lung microvascular permeability after microembolization in sheep. Circ. Res. **48:**344–351.
18. **Fruchtman, S. M., M. E. Gombert, and H. A. Lyons.** 1983. Adult respiratory distress syndrome as a cause of death in pneumococcal pneumonia. Report of ten cases. Chest **83:**598–601.
19. **Fox, G. A., and D. G. McCormack.** 1992. The pulmonary physician and critical care. A new look at the pulmonary circulation in acute lung injury. Thorax **47:**743–747.
20. **Gadek, J. E.** 1992. Adverse effects of neutrophils on the lung. Am. J. Med. **92:**27S-31S.
21. **Geelen, S., C. Bhattacharyya, and E. Tuomanen.** 1992. Induction of procoagulant activity on human endothelial cells by *Streptococcus pneumoniae*. Infect. Immun. **60:**4179–4183.
22. **Geelen, S., C. Bhattacharyya, and E. Tuomanen.** 1993. The cell wall mediates pneumococcal attachment to and cytopathology in human endothelial cells. Infect. Immun. **61:**1538–1543.
23. **Goodman, B. E., and E. D. Crandall.** 1982. Dome formation in primary cultured monolayers of alveolar epithelial cells. Am. J. Physiol. **243:**C96–C100.
24. **Goodman, B. E., R. S. Fleischer, and E. D. Crandall.** 1983. Evidence for active Na+ transport by cultured monolayers of pulmonary alveolar epithelial cells. Am. J. Physiol. **245:**C78-C83.
25. **Gorin, A. B., and P. A. Stewart.** 1979. Differential permeability of endothelial and epithelial barriers to albumin flux. J. Appl. Physiol. **47:**1315–1324.
26. **Green, T. P., D. E. Johnson, R. P. Marchessault, and C. W. Gatto.** 1988. Transvascular flux and tissue accrual of Evans blue: effects of endotoxin and histamine. J. Lab. Clin. Med. **111:**173–183.
27. **Harlan, J. M.** 1985. Leukocyte-endothelial interactions. Blood **65:**513–525.
28. **Haschek, W. M., K. M. Reiser, A. J. Klein-Szanto, J. P. Kehrer, L. H. Smith, J. A. Last, and H. P. Witschi.** 1983. Potentiation of butylated hydroxytoluene-induced acute lung damage by oxygen. Cell kinetics and collagen metabolism. Am. Rev. Respir. Dis. **127:**28–34.
29. **Heussel, C. P., H. U. Kauczor, G. Heussel, B. Fischer, P. Mildenberger, and M. Thelen.** 1997. Early detection of pneumonia in febrile neutropenic patients: use of thin-section CT. Am. J. Roentgenol. **169:**1347–1353.
30. **Kapanci, Y., E. R. Weibel, H. P. Kaplan, and F. R. Robinson.** 1969. Pathogenesis and reversibility of the pulmonary lesions of oxygen toxicity in monkeys. II. Ultrastructural and morphometric studies. Lab. Investig. **20:**101–118.
31. **Laufe, M. D., R. H. Simon, A. Flint, and J. B. Keller.** 1986. Adult respiratory distress syndrome in neutropenic patients. Am. J. Med. **80:**1022–1026.
32. **Martin, C., L. Papazian, M. J. Payan, P. Saux, and F. Gouin.** 1995. Pulmonary fibrosis correlates with outcome in adult respiratory distress syndrome. A study in mechanically ventilated patients. Chest **107:**196–200.
33. **Maunder, R. J., R. C. Hackman, R. Riff, R. K. Albert, and S. C. Springmeyer.** 1986. Occurrence of the adult respiratory distress syndrome in neutropenic patients. Am. Rev. Respir. Dis. **133:**313–316.
34. **Nelson, S., A. M. Heyder, J. Stone, M. G. Bergeron, S. Daugherty, G. Peterson, N. Fotheringham, W. Welch, S. Milwee, and R. Root.** 2000. A randomized controlled trial of Filgrastim for the treatment of hospitalized patients with multilobar pneumonia. J. Infect. Dis. **182:**970–973.
35. **Ognibene, F. P., S. E. Martin, M. M. Parker, T. Schlesinger, P. Roach, C. Burch, J. H. Shelhamer, and J. E. Parrillo.** 1986. Adult respiratory distress syndrome in patients with severe neutropenia. N. Engl. J. Med. **315:**547–551.
36. **Paine, R., M. W. Rolfe, T. J. Standiford, M. D. Burdick, B. J. Rollins, and R. M. Strieter.** 1993. MCP-1 expression by rat type II alveolar epithelial cells in primary culture. J. Immunol. **150:**4561–4570.
37. **Perlino, A., and D. Rimland.** 1985. Alcoholism, leukopenia, and pneumococcal sepsis. Am. Rev. Respir. Dis. **132:**757–760.
38. **Rich, A. R., and C. M. McKee.** 1939. The pathogenicity of avirulent pneumococci for animals deprived of leukocytes. Bull. Johns Hopkins Hosp. **64:**343–346.
39. **Sakuma, T., G. Okaniwa, T. Nakada, T. Nishimura, S. Fujimura, and M. A. Matthay.** 1994. Alveolar fluid clearance in the resected human lung. Am. J. Respir. Crit. Care Med. **150:**305–310.
40. **Sato, S., N. Ouellet, I. Pelletier, M. Simard, A. Rancourt, M. G. Bergeron.** 2002. Role of galectin-3 as an adhesion molecule for neutrophil extravasation during streptococcal pneumonia. J. Immunol. **168:**1813–1822.
41. **Shasby, D. M., S. S. Shasby, and M. J. Peach.** 1983. Granulocytes and phorbol myristate acetate increase permeability to albumin of cultured endothelial monolayers and isolated perfused lungs. Role of oxygen radicals and granulocyte adherence. Am. Rev. Respir. Dis. **127:**72–76.
42. **Simon, R. H., and R. Paine.** 1995. Participation of pulmonary alveolar epithelial cells in lung inflammation. J. Lab. Clin. Med. **126:**108–118.
43. **Sivan, Y., C., Mor, S. Jundi, and C. J. Newth.** 1990. Adult respiratory distress syndrome in severely neutropenic children. Pediatr. Pulmonol. **8:**104–108.
44. **Standiford, T. J., S. L. Kunkel, M. A. Basha, S. W. Chensue, J. P. Lynch, G. B. Toews, J. Westwick, and R. M. Strieter.** 1990. Interleukin-8 gene expression by a pulmonary epithelial cell line. A model for cytokine networks in the lung. J. Clin. Investig. **86:**1945–1953.
45. **Takizawa, H.** 1998. Airway epithelial cells as regulators of airway inflammation. Int. J. Mol. Med. **1:**367–378.
46. **Tate, R. M., and J. E. Repine.** 1983. Neutrophils and the adult respiratory distress syndrome. Am. Rev. Respir. Dis. **128:**552–559.
47. **Toews, G. B.** 1999. Cellular alterations in fibroproliferative lung disease. Chest **116b:**112S-116S.
48. **Vansteenkiste, J. F., and M. A. Boogaerts.** 1989. Adult respiratory distress syndrome in neutropenic leukemia patients. Blut **58:**287–290.
49. **Wang, E., M. Simard, Y. Bergeron, D. Beauchamp, and M. G. Bergeron.** 2000. In vivo activity and pharmacokinetics of ziracin (SCH27899), a new long-acting everninomicin antibiotic, in a murine model of penicillin-susceptible and penicillin-resistant pneumococcal pneumonia. Antimicrob. Agents Chemother. **44:**1010–1018.
50. **Wang, E., M. Simard, N. Ouellet, Y. Bergeron, D. Beauchamp, and M. G. Bergeron.** 2000. Modulation of cytokines and chemokines, limited pulmonary vascular bed permeability, and prevention of septicemia and death with ceftriaxone and interleukin-10 in pneumococcal pneumonia. J. Infect. Dis. **182:**1255–1259.
51. **Wang, E., N. Ouellet, M. Simard, I. Fillion, Y. Bergeron, and M. G. Bergeron.** 2001. Host response to *Streptococcus pneumoniae* and *Klebsiella pneumoniae* bacteremia in mice. Infect. Immun. **69:**5294–5304.

52. **Weiland, J. E., W. B. Davis, J. F. Holter, J. R. Mohammed, P. M. Dorinsky, and J. E. Gadek.** 1986. Lung neutrophils in the adult respiratory distress syndrome. Clinical and pathophysiologic significance. Am. Rev. Respir. Dis. **133:**218–225.

53. **Weiss, S. J.** 1989. Tissue destruction by neutrophils. N. Engl. J. Med. **320:** 365–376.

54. **Winternitz, M. C., and A. D. Hirschfelder.** 1913. Studies upon experimental pneumonia in rabbits. J. Exp. Med. **17:**657–665.

55. **Xie, J., R. Li, P. Kotovuori, C. Vermot-Desroches, J. Wijdenes, M. A. Arnaout, P. Nortamo, and C. G. Gahmberg.** 1995. Intercellular adhesion molecule-2 (CD102) binds to the leukocyte integrin CD11b/CD18 through the A domain. J. Immunol. **155:**3619–3628.